

## Late stage functionalization via Chan-Lam amination: rapid access to potent and selective integrin inhibitors

Henry Robinson,<sup>[a]</sup> Steven A. Oatley,<sup>[b]</sup> James E. Rowedder,<sup>[c]</sup> Pawel Slade,<sup>[c]</sup> Simon J. F. Macdonald,<sup>[c]</sup> Stephen P. Argent,<sup>[b]</sup> Jonathan D. Hirst,<sup>[b]</sup> Thomas McInally<sup>[a]</sup> and Christopher J. Moody<sup>\*[b]</sup>

[a] School of Chemistry  
The GSK Carbon Neutral Laboratories for Sustainable Chemistry University of Nottingham  
Jubilee Campus, Triumph Road  
Nottingham NG7 2TU, U.K.

[b] School of Chemistry  
University of Nottingham, University Park  
Nottingham NG7 2RD, U.K.  
\*Email: c.j.moody@nottingham.ac.uk

[c] Medicinal Science & Technology  
GlaxoSmithKline Medicines Research Centre  
Gunnels Wood Road, Stevenage, SG1 2NY, U.K

**Abstract:** A late stage functionalization of the aromatic ring in amino acid derivatives is described. The key step is a copper-catalysed diversification of a boronate ester by amination (Chan-Lam reaction) that can be carried out on a complex  $\beta$ -aryl- $\beta$ -amino acid scaffold, and not only considerably extends the substrate scope of amination partners, but also delivers an array of potent and selective integrin inhibitors as potential treatments of idiopathic pulmonary fibrosis (IPF). This versatile chemistry strategy, which is amenable to high throughput array protocols, allows the installation of pharmaceutically valuable heteroaromatic fragments at a late stage by direct coupling to the NH heterocycles, leading to compounds with drug-like attributes, and is a useful addition to the medicinal chemist's repertoire.

### Introduction

Late stage functionalization (LSF) is a powerful tool in medicinal chemistry that enables rapid generation of highly diverse drug-like molecules from complex intermediates. This reduces overall step count, improving time and cost efficiency whilst maximizing diversity of chemical space exploration in lead optimization to elucidate structure-activity-relationships (SAR). The most frequently used reactions within medicinal chemistry are amide bond formations, Suzuki-Miyaura couplings, Buchwald-Hartwig couplings and  $S_NAr$  reactions.<sup>[1]</sup> They are effective tools for introducing diversity, but are often unsuitable for LSF, due to forcing reaction conditions such as high temperatures, strong bases, expensive catalysts and complex ligands. On the other hand, C-H activation to install a variety of structural motifs at a late stage is a preferred tactic, although notwithstanding recent advances,<sup>[2]</sup> methods remain somewhat limited.

Despite the fact that nitrogen-containing heterocycles are amongst the most prevalent cyclic structural features in small drug molecules, there are few examples of mild and robust aromatic C-N bond formation methods.<sup>[2]</sup> This is particularly pertinent for the installation of heteroaromatic 5-membered rings by direct coupling of the corresponding NH heterocycle, and therefore, methodology that is tolerant of a range of functional groups, but would allow the installation of these pharmaceutically valuable structural features at a late stage would be a welcome addition to the medicinal chemist's inventory.<sup>[3]</sup>

First reported in 1997,<sup>[4–6]</sup> the Chan-Lam amination that formally involves the coupling of two nucleophilic species has been characterized as capricious,<sup>[7]</sup> with the more commonplace Buchwald-Hartwig and Ullmann nucleophile-electrophile couplings subsequently gaining prominence in drug discovery.<sup>[1,8,9]</sup> However, due to limited substrate scope and harsh reaction conditions, neither of these are a viable methodology for LSF. In 2017, the mechanism of the Chan-Lam amination was elegantly elucidated by Vantourout *et al.*<sup>[10]</sup> The substrate scope, including both alkyl and aryl amines, and the improved reliability of the reaction, including its use in the synthesis of imatinib by a late stage amination,<sup>[10]</sup> thereby marked it as a potential methodology for LSF. Herein we report the first example of a more strategic LSF in drug discovery employing the Chan-Lam amination reaction that not only considerably extends the substrate scope of *N*-coupling partners, but also delivers an array of potent, selective (particularly vs.  $\alpha_v\beta_1$ ) and drug-like  $\alpha_v\beta_6$  integrin inhibitors as potential treatments of idiopathic pulmonary fibrosis (IPF).

IPF is a chronic interstitial lung disease, characterized by excessive scarring of the interstitium. The incidence of IPF is estimated to be 4.6 per 100,000 and 6.8 per 100,000 in the UK and the USA, respectively, with >5,000 and >14,000 people diagnosed each year.<sup>[11–13]</sup> IPF is fatal, with median survival rates of between two and four years.<sup>[13,14]</sup> Currently there are two approved treatments for the disease: pirfenidone **1** and nintedanib **2** (Figure 1). Both reduce the rate of lung function decline, although neither fully halts disease progression and various side effects are attributed to their use, leading to poor patient compliance.<sup>[15]</sup>

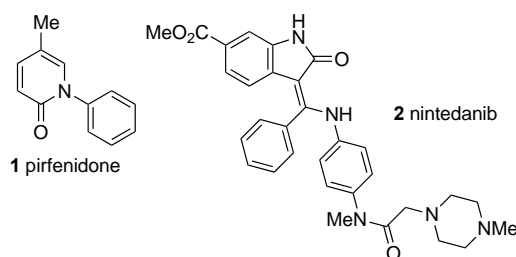


**Figure 1.** Compounds used in the treatment of IPF; pirfenidone **1** and nintedanib **2**.

Transforming growth factor-beta (TGF- $\beta$ ) is a key agent in the activation of fibroblasts,<sup>[16]</sup> the cells responsible for collagen deposition and the resulting build-up of scar tissue associated with IPF. Whilst direct inhibition of TGF- $\beta$  can lead to serious health complications,<sup>[17]</sup> it can be modulated sufficiently by inhibition of specific integrins. Integrins are heterodimeric cell surface receptors, composed of an  $\alpha$  and  $\beta$  subunit, that play roles in many cell adhesion processes.<sup>[18]</sup> A subset of eight integrins, from a total of 24 in vertebrates, recognize an arginine-glycine-aspartic acid (RGD) sequence motif in the latency associated peptide (LAP) that maintains a TGF- $\beta$  in an inactive form.<sup>[19]</sup> At least two of these integrins, namely  $\alpha_v\beta_6$  and  $\alpha_v\beta_8$ , activate TGF- $\beta$  by binding to the LAP (Figure 2), and expression of the  $\alpha_v\beta_6$  integrin in particular is elevated in IPF lung tissue compared to healthy tissue.<sup>[20]</sup> Thus, selective inhibition of this integrin, for example vs.  $\alpha_v\beta_1$  and  $\alpha_v\beta_3$ , is an attractive therapeutic strategy.<sup>[19]</sup>

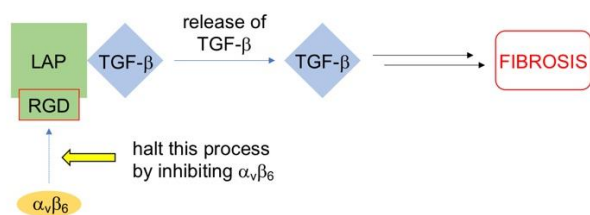


**Figure 2.** Inhibition of the  $\alpha_v\beta_6$  integrin binding to LAP prevents the activation of TGF- $\beta$ .<sup>[20,21]</sup>

Recently, an  $\alpha_v\beta_6$  antibody and the GSK candidate GSK3008348 **3** have both been evaluated clinically,<sup>[22]</sup> and inhibition of the  $\alpha_v\beta_6$  integrin with **3** did not cause any adverse effects in healthy volunteers when dosed with 3-3000  $\mu\text{g}$ .<sup>[23]</sup> Inhibitor **3**, and structurally similar compounds, are RGD mimetics, and such structures form the basis of our current work.

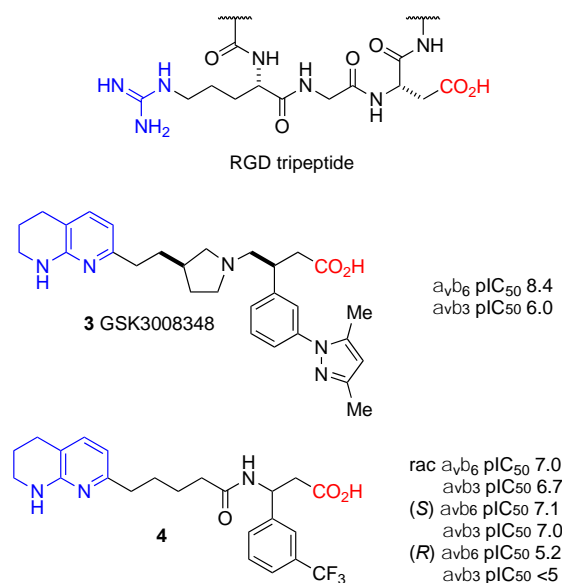


**Figure 3.** The RGD tripeptide sequence, the clinical candidate **3** and the starting point for the current work, the pan-integrin inhibitor **4**. Compounds are colored to show the structural similarities that mimic the basic and acidic sites in the RGD sequence by compounds **3** and **4**. Selectivity and potency data from cell adhesion assays are shown.<sup>[24,25]</sup>

Previous work in our group led to the development of a pan integrin inhibitor, the 3- $\text{CF}_3$ -substituted- $\beta$ -aryl- $\beta$ -amino acid derivative **4**, pan in this case referring to the fact that compound **4** exhibits broadly similar levels of potency towards multiple integrins.<sup>[24]</sup> Whilst compound (S)-**4** displayed appropriate physicochemical properties (ChromLogD 2.73, permeability >100 nm/s, aqueous solubility >300  $\mu\text{M}$ ) and was therefore considered as lead-like, comparison with GSK3008348 **3**, and other analogues,<sup>[26,27]</sup> revealed significant differences in potency and selectivity (Figure 3). Therefore, in order to investigate whether the incorporation of an *N*-linked heterocycle resulted in increased potency in our own series, we set out to synthesize an array of analogues of the antagonist **4**, using Chan-Lam amination LSF as the cornerstone of our strategy.

## Results and Discussion

Of the two enantiomers of the  $\text{CF}_3$ -compound **4**, the activity has been demonstrated to reside in the (S)-enantiomer (Figure 3), and therefore the new *N*-linked analogues were only prepared as the (S)-enantiomer as shown in Scheme 1. Methodology

reported by Ellman *et al.* was used to generate the (*S*)- $\alpha$ -aminoester precursor *via* titanium tetra-isopropoxide mediated condensation of (*R*)-*tert* butyl sulfinamide with 3-bromobenzaldehyde **5** to give (*R*)-sulfinimine **6**, and subsequent Reformatsky reaction to give **7**.<sup>[28]</sup> The Reformatsky reagent was formed *in situ* *via* treatment of *tert*-butyl bromoacetate with TMSCl activated zinc dust, generating the organozinc enolate. The pre-prepared sulfinimine **6** was subsequently added following cooling to 0 °C, to minimize formation of the double addition product **8** (Scheme 1).<sup>[29]</sup> The (*S*)-stereochemistry of the newly formed stereocentre in **7** was confirmed by X-ray crystallography (Figures 4 and S1, Supporting Information), and is in accord with that expected from the work reported by Ellman *et al.*<sup>[28]</sup> After selective removal of the sulfinamide functionality under acidic conditions, the amide **11** was formed by T3P mediated coupling of **9**<sup>[30]</sup> with the Boc-protected-tetrahydro-1,8-naphthyridine-pentanoic acid **10**, the preparation of which is described in the literature.<sup>[31]</sup> The Boc-protecting group was chosen so that it could be removed in concert with the *tert*-butyl ester after performing the array chemistry (*q.v.*). The key boronate intermediate **12** was prepared in excellent yield from Miyaura borylation of **11** (Scheme 1).

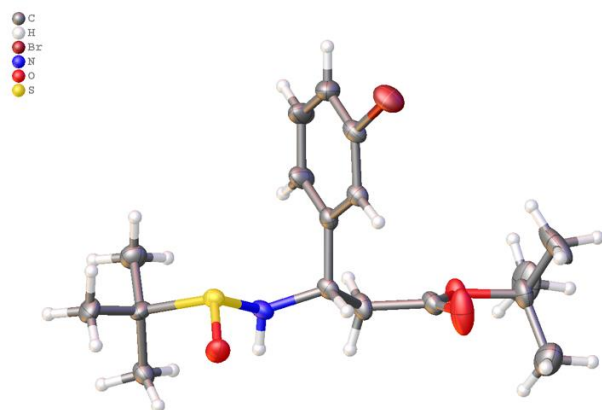
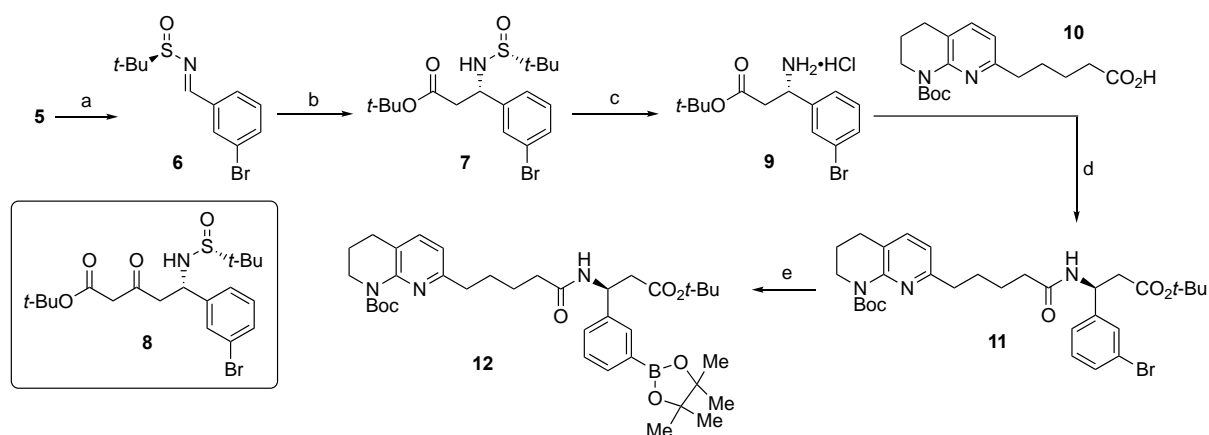


**Figure 4.** X-Ray crystal structure of *tert*-butyl (*S*)-3-(3-bromophenyl)-3-(((*R*)-*tert*-butylsulfinyl)amino)propanoate **7**.



**Scheme 1.** Synthesis of key boronate intermediate **12**. *Reagents and Conditions:* a) (*R*)-*tert*-butyl sulfinamide, Ti(OiPr)<sub>4</sub>, THF, rt; b) i) Zn, TMSCl, *tert*-butyl bromoacetate, THF, N<sub>2</sub>, reflux ii) 0 °C; c) HCl (4 M in 1,4-dioxane), diethyl ether, rt, 85% over three steps; d) **10**, T3P, *i*-Pr<sub>2</sub>NEt, acetonitrile, 0 °C, 86%; e) B<sub>2</sub>Pin<sub>2</sub>, KOAc, Pd(dppf)Cl<sub>2</sub>.CH<sub>2</sub>Cl<sub>2</sub>, 1,4-dioxane, 80 °C, N<sub>2</sub>, 90%. T3P = propanephosphonic acid anhydride.

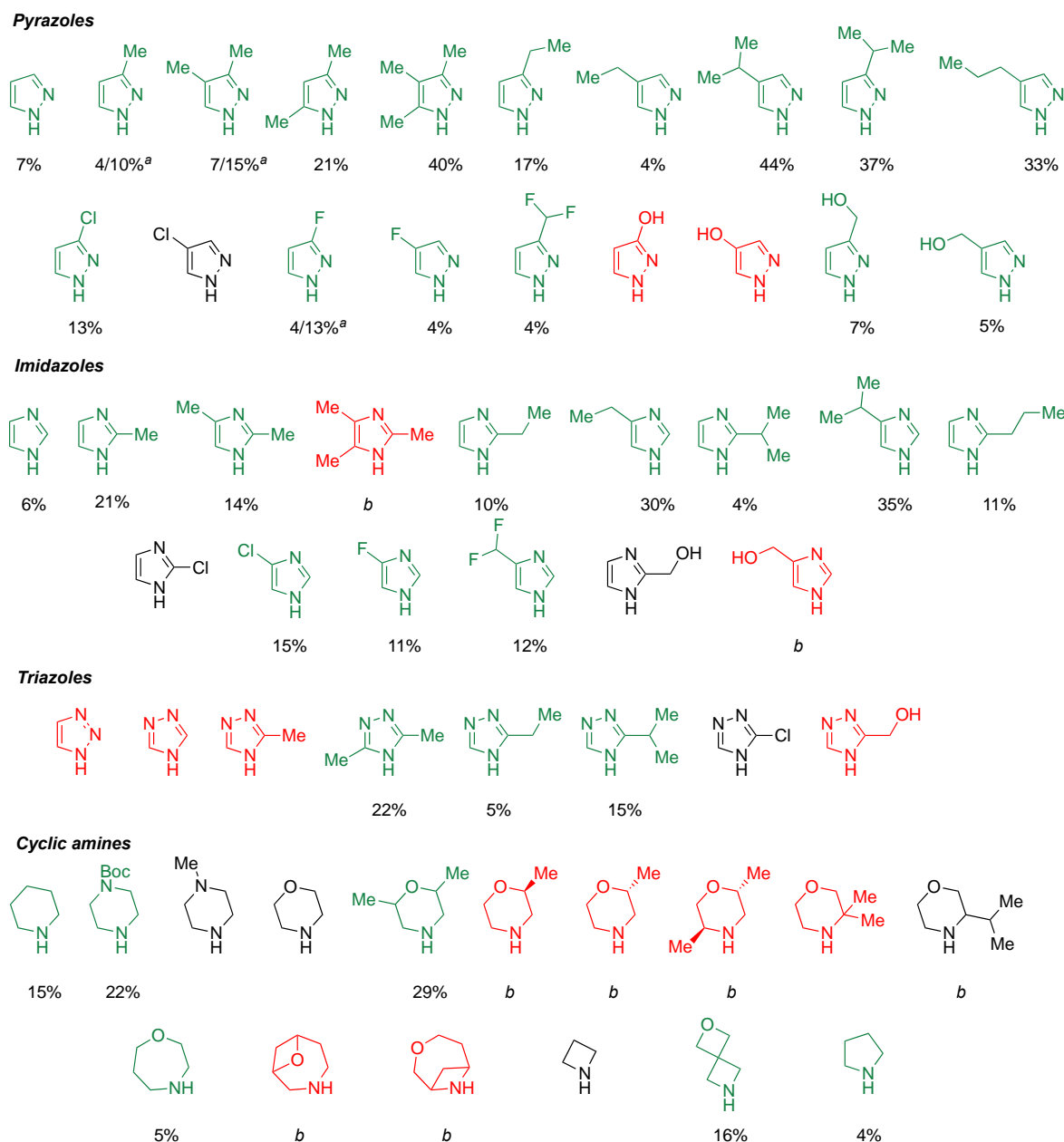
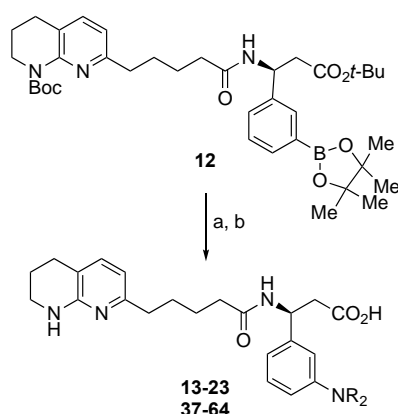


**Figure 5.** Diversity of monomer amine coupling partners. Structures of pyrazoles, imidazoles, triazoles and cyclic secondary amines used in the Chan-Lam coupling reactions. Monomers are highlighted according to reaction outcome: green = successful coupling and product isolation; yields after mass-directed auto purification (MDAP); black = successful coupling but unsuccessful product isolation; red = unsuccessful coupling. *a* = yields of the separated regioisomers; *b* = amine used as the hydrochloride salt.

A range of 58 highly diverse heteroaromatic (19 pyrazoles, 15 imidazoles, 8 triazoles) and 16 cyclic secondary amines (Figure 5) was selected to provide thorough exploration of chemical space within the specificity determining loop (SDL) in the integrin binding site.<sup>[22]</sup> Amines that would allow comparison between the resulting array compounds by single point changes were selected. Substituents within the amines were intentionally kept simple due to the lack of available SAR and therefore included small alkyl groups, halides and polar and non-polar hydrogen bond donors. To the best of our knowledge, there are few representative examples of Chan-Lam aminations using small heteroaromatic NH compounds in the literature; those that are

reported incorporate unsubstituted pyrazole, imidazole and benzimidazole parent rings.<sup>[6,10,32]</sup>

The *N*-linked heterocyclic analogues were prepared in a high throughput array format. Reactions were performed in parallel in 4 mL vials in a 6 x 4 block placed upon a hotplate (see Supporting Information, General Preparation A), and utilized mass-directed auto purification (MDAP) to allow rapid generation of diverse compounds to develop meaningful SARs. The inhibitor analogues were prepared *via* Chan-Lam amination between the boronate **12** and the selected amines on a 0.10 mmol scale, followed by global deprotection of both *tert*-butyl-based groups with TFA and subsequent isolation *via* MDAP (Scheme 2). Although isolated yields were often poor (<20%), this is due to the high UV threshold used by the MDAP method to maximize the chances of obtaining sample with high purity, which frequently results in significant loss of material. The yields of the Chan-Lam coupling were improved (45-52%) when the reaction was carried out on larger scale in batch format, albeit on the ethyl ester analogue of boronate **12**, as described below for the coupling reactions of 3-chloro- and 3-isopropyl-pyrazoles and for piperidine. In the case of unsymmetrical heterocycles, two or more regioisomeric products can be formed and generally, the major regioisomer resulted from Chan-Lam coupling at the least sterically hindered nitrogen. In most cases, the major regioisomer was successfully separated from the minor regioisomer *via* MDAP, although some analogues were isolated as mixtures (see Supporting Information). Regioisomers were distinguishable by HSQCME NMR (see Supporting Information).



**Scheme 2.** Array synthesis of integrin antagonists. *Reagents and Conditions:* a) N-H compounds (2.5 eq), Cu(OAc)<sub>2</sub> (1 eq), B(OH)<sub>3</sub> (2 eq), acetonitrile, 3 Å MS, 70 °C; b) TFA, CH<sub>2</sub>Cl<sub>2</sub>, rt, 4-44% after MDAP purification. Structures of compounds **13-23** shown in Table 1; structures **37-64** shown in the Supporting Information.

From the array of 58 NH coupling partners, 39 samples of sufficient purity (>85% by LCMS) for biological evaluation were isolated *via* MDAP (shown in green in Figure 5) (for details, see Supporting Information), including the minor regioisomer analogues from reaction with 3-methyl-, 3-fluoro- and 3,4-dimethyl-pyrazoles. Despite desired product being detected via LC/MS, the isolation of eight analogues via MDAP was unsuccessful (shown in black in Figure 5). The Chan-Lam coupling reaction did not proceed with 14 of the selected monomers shown in red in Figure 5. Monomers that failed to react were often structurally similar; these were monomers containing a heteroatom that was β to the reactive N-H, the majority of triazoles and most monomers that contained an unprotected hydroxyl group. It is thought that the failed reactions that fit into the first two descriptors were unsuccessful due to reduced Lewis basicity of the monomers that is known to be an important factor within the Chan-Lam

reaction.<sup>[10]</sup> The monomers containing hydroxyl groups likely failed due to a competing reaction between the N-H and O-H, leading to a reduced reaction rate and subsequent increase in the rate of protodeborylation and phenol formation by oxidation.<sup>[10]</sup> Nevertheless, the range of heteroaromatic coupling partners available for use in the Chan-Lam reaction has been considerably extended.

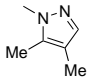
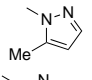
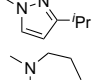
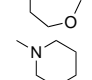
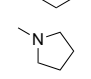
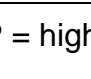
With an array of potential integrin antagonists in hand, cell adhesion assays ( $n = 2$ ) were used to assess the potency and selectivity against  $\alpha_v\beta_1$ ,  $\alpha_v\beta_3$  and  $\alpha_v\beta_6$  integrins, measuring the ability of compounds to inhibit the binding of the integrin (expressed on the surface of cells) to the endogenous peptide ligand.<sup>[33]</sup> The upper limit of the assay for  $\alpha_v\beta_6$  is  $pIC_{50}$  8.6 – 8.7, and a difference of more than 0.4 log units in compound potency is regarded as significant. Lipophilicity of the compounds was also determined by measuring the logD at pH7.4 chromatographically (ChromLogD pH7.4),<sup>[34]</sup> whilst high throughput permeability (HTP) was determined by the Parallel Artificial Membrane Permeation Assay (PAMPA).<sup>[35]</sup> Data for selected compounds **13-23** are shown in Table 1.

Related pyrazoles and imidazoles, for example the parent heterocycles and their mono-chloro derivatives, generally display similar levels of potency and selectivity, as demonstrated by **13-16**, but differ in their high throughput permeability (HTP nm/s); each of the imidazole analogues analysed suffer from poor permeability, whereas the pyrazole analogues display modest to good permeability. This is due to the increased basicity of imidazoles compared to pyrazoles, leading to more basic and polar compounds that are considerably less permeable. This is supported by the observation that each pyrazole analogue exhibits a ChromLogD value that is at least 0.6 log units greater than the corresponding imidazole analogue. Within the pyrazole series, comparison of **19** (5-methyl), **17** (3,5-dimethyl) and **18** (4,5-dimethyl) suggests that substitution at the 3 position,  $\alpha$  to the  $sp^2$  nitrogen can provide an improvement in selectivity for the  $\alpha_v\beta_6$  integrin over the  $\alpha_v\beta_3$  integrin, with 4 and 5 substitution providing no obvious advantage on either the potency or selectivity. The aliphatic amine analogues are generally less potent towards the  $\alpha_v\beta_6$  integrin, with the exception of the piperidine analogue **22** which appears to be a potent  $\alpha_v\beta_3$  and  $\alpha_v\beta_6$  inhibitor.

**Table 1.** A selection of N-linked analogues illustrating the SAR.<sup>[a]</sup>

**13-23**

No.	-NR <sub>2</sub>	$pIC_{50}$ $\alpha_v\beta_6$	$pIC_{50}$ $\alpha_v\beta_3$	$pIC_{50}$ $\alpha_v\beta_1$	ChromLogD pH7.4	HTP nm/s
<b>13</b>		7.8	7.4	6.0	1.83	22
<b>14</b>		7.9	7.2	6.2	1.23	3
<b>15</b>		7.8	6.8	5.8	1.92	3
<b>16</b>		8.0	6.8	6.3	2.61	86
<b>17</b>		7.9	6.8	6.7	2.33	19.5

<b>18</b>		7.3	7.0	-	2.65	17
<b>19</b>		7.6	7.3	-	2.17	13
<b>20</b>		7.7	7.1	6.5	3.22	120
<b>21</b>		6.7	7.7	6.5	1.98	3
<b>22</b>		7.7	7.6	6.4	2.85	73
<b>23</b>		7.3	7.6	6.4	2.84	88

[a] HTP = high throughput permeability.

The 3-chloro pyrazole analogue **16** was identified as a suitably lead-like compound, with high potency and excellent selectivity for  $\alpha_v\beta_6$  over  $\alpha_v\beta_3$  of 1.2 log units together with good permeability. This compound, along with the most permeable analogue, the 3-isopropyl pyrazole derivative **20** and the aliphatic amine analogue with the highest potency towards  $\alpha_v\beta_6$  (**22**), were selected for further drug metabolism and pharmacokinetics (DMPK) studies. Thus, compounds **16**, **20** and **22** were resynthesized on a larger scale using a modified route utilizing ethyl bromoacetate in the Reformatsky reaction rather than the *tert*-butyl ester, and installation of the heterocycles at an earlier stage (Scheme S1, Supporting Information). The three relevant Chan-Lam reactions were performed on 0.95 mmol scale, giving moderate yields ranging from 45-56%. On this larger scale, the minor 5-isopropylpyrazole regioisomer was isolated separately to the major regioisomer and the resulting combined yield was 77%. These compounds were *N*-deprotected and immediately subjected to amide coupling conditions with T3P. Following this, the compounds were subsequently *N*-deprotected and saponified to give the desired analogues **16**, **20** and **22**.

Initial DMPK studies reveal that *in vitro* these compounds have acceptable permeability and metabolic stability that complement their measured potency and selectivity profiles, further enhancing their potential as drug-like lead compounds (Tables S1 and S2, Supporting Information). For example, the piperidine analogue **22** exhibits a moderate passive permeability ( $P_{app} = 9.7$ ) and an efflux ratio of 8.2, and stability to Phase 1 metabolism in human liver microsomes, with a half-life of greater than 8 h. The additional data for piperidine **22** (Table S2) suggest that it, and related analogues, may have oral bioavailability.

As one of the most selective compounds, 3-chloropyrazole **16** was docked into the  $\alpha_v\beta_6$  and  $\alpha_v\beta_3$  crystal structures (4UM9 and 1L5G respectively) to generate binding poses that would rationalize the selectivity (Figure 6).<sup>[36,37]</sup>



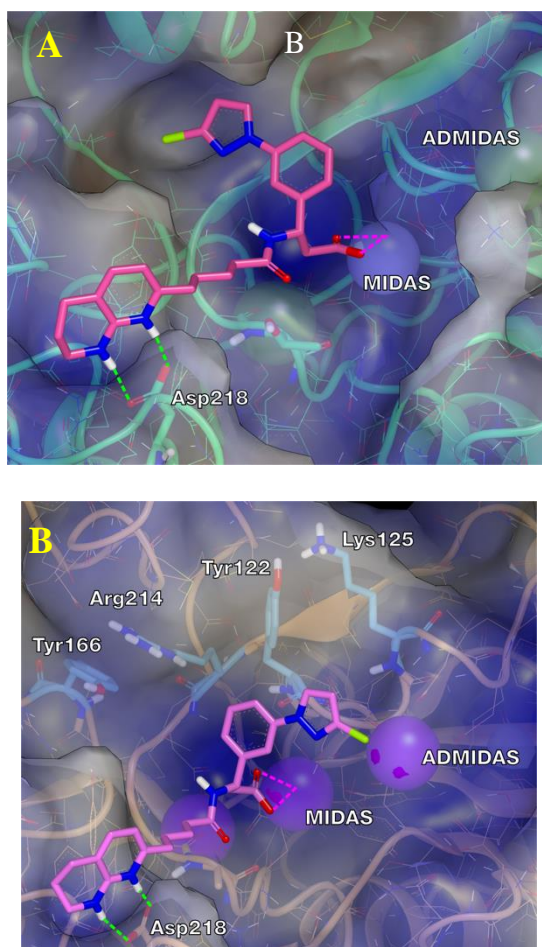


**Figure 6.** Docked poses of 3-chloropyrazole analogue **16** in the  $\alpha_v\beta_6$  and  $\alpha_v\beta_3$  crystal structure (**A** and **B** respectively). Conformers were generated using OMEGA and subsequent docking was performed using FRED.<sup>[38,39]</sup> Visualization of conformers was performed using VIDA. The surface of the binding site is overlaid to show hydrophobicity; lighter areas are more hydrophobic and blue areas are more hydrophilic. Hydrogen bonds are displayed as dashed lines, showing coordination between the 1,8-tetrahydronaphthyridine and Asp218, and the carboxylate with the metal ion in the metal ion dependent adhesion site (MIDAS). ADMIDAS = adjacent metal ion dependent adhesion site.

Figure 6A shows the specificity determining loop (SDL) in the  $\alpha_v\beta_6$  binding site is relatively open and able to accommodate the chloro-pyrazole substituent. In contrast, Figure 6B, shows that there are four sidechains (labelled) in the  $\alpha_v\beta_3$  integrin SDL that close off this pocket, preventing **16** binding in the conformation seen with  $\alpha_v\beta_6$  integrin, with Tyr166 and Arg214 being particularly influential. These residues limit the size of the pocket, and thus force the heterocyclic substituent into a more solvent exposed position, reducing overall binding affinity. Additionally, in this more solvent exposed position, the ADMIDAS manganese ion in the crystal structure of  $\alpha_v\beta_3$  clashes with the chlorine atom in the pyrazole motif, further impacting binding affinity. In combination, these factors lead to the improved selectivity that is observed between the unsubstituted pyrazole **13** and those pyrazole analogues that contain a 3-substituent (**16**, **17** and **18**).

## Conclusion

In conclusion, we have developed a late stage diversification of a complex, drug-like scaffold using a Chan-Lam copper catalyzed amination reaction. The key  $\beta$ -aryl- $\beta$ -amino acid coupling partner was readily prepared on 15 g scale employing a

stereoselective Reformatsky addition to a sulfinimine, followed by Miyaura borylation to install the required pinacol borane motif. Subsequent Chan-Lam amination using an array of diverse and functionalized NH components led to the isolation and biological evaluation of a wide range of analogues. The compounds are potent  $\alpha_v\beta_6$  integrin antagonists, and show some selectivity particularly vs.  $\alpha_v\beta_1$ , with sufficiently acceptable permeability and metabolic stability to be considered as lead compounds for drug development. Our results extend the earlier work of Vantourout *et al.*<sup>[10]</sup> and establish a versatile strategy in a medicinal chemistry setting, which is amenable to high throughput array protocols. This thereby allows the installation of pharmaceutically valuable heteroaromatic fragments at a late stage by direct coupling to the NH heterocycles, leading to compounds with drug-like attributes, and is a useful addition to the medicinal chemist's repertoire.

### Acknowledgements

We acknowledge GlaxoSmithKline (GSK) for financial support (part-studentship to H.R.); S.A.O. is supported by EPSRC [EP/P510592/1] under a GlaxoSmithKline CASE award scheme. We thank GSK colleagues Sean Lynn and Heather Barnett for their help with NMR spectroscopy and array chemistry respectively, Ashley Hancock for his assistance with purchasing reagents, and Cassie Pratley for her help with laboratory orientation and assistance. We thank Reach Separations for providing e.e. determinations, OpenEye Scientific Software, Inc. for providing academic licenses to their software, and Sygnature Discovery for performing DMPK analyses. We acknowledge the use of JChem for Excel (version 18.23.0.370) (ChemAxon <https://www.chemaxon.com>) and DataWarrior to visualize structures and data.

### Conflicts of Interest

The authors declare no conflicts of interest. HR, JER, SJFM and CJM are shareholders in GSK.

**Keywords:**  $\beta$ -amino acids • C-N coupling • integrin antagonists • late stage functionalization • medicinal chemistry

### References

- [1] D. G. Brown, J. Boström, *J. Med. Chem.* **2016**, *59*, 4443–4458.
- [2] T. Cernak, K. D. Dykstra, S. Tyagarajan, P. Vachal, S. W. Krska, *Chem. Soc. Rev.* **2016**, *45*, 546–576.
- [3] A. R. D. Taylor, M. Maccoss, A. D. G. Lawson, *J. Med. Chem.* **2013**, *57*, 5845–5859.
- [4] D. M. T. Chan, K. L. Monaco, R. P. Wang, M. P. Winters, *Tetrahedron Lett.* **1998**, *39*, 2933–2936.
- [5] D. A. Evans, J. L. Katz, T. R. West, *Tetrahedron Lett.* **1998**, *39*, 2937–2940.
- [6] P. Y. S. Lam, C. G. Clark, S. Saubern, J. Adams, M. P. Winters, D. M. T. Chan, A. Combs, *Tetrahedron Lett.* **1998**, *39*, 2941–2944.
- [7] D. J. Cundy, S. A. Forsyth, *Tetrahedron Lett.* **1998**, *39*, 7979–7982.
- [8] D. Ma, Q. Cai, H. Zhang, *Org. Lett.* **2003**, *5*, 2453–2455.
- [9] S. M. Mennen, C. Alhambra, C. L. Allen, M. Barberis, S. Berritt, T. A. Brandt, A. D. Campbell, J. Castanon, A. H. Cherney, M. Christensen, D. B. Damon, J. Eugenio de Diego, S. García-Cerrada, P. Garcia-Losada, R. Haro, J. M. Janey, D. C. Leitch, L. Li, F. Liu, et al., *Org. Process Res. Dev.* **2019**, DOI 10.1021/acs.oprd.9b00140.
- [10] J. C. Vantourout, H. N. Miras, A. Isidro-Llobet, S. Sproules, A. J. B. Watson, *J. Am. Chem. Soc.* **2017**, *139*, 4769–4779.
- [11] J. Gribbin, R. B. Hubbard, I. Le Jeune, C. J. P. Smith, J. West, L. J. Tata, *Thorax* **2006**, *61*, 980–985.
- [12] G. Raghu, D. Weycker, J. Edelsberg, W. Z. Bradford, G. Oster, *Am. J. Respir. Crit. Care Med.* **2006**, *174*, 810–816.

- [13] V. Navaratnam, K. M. Fleming, J. West, C. J. P. Smith, R. G. Jenkins, A. Fogarty, R. B. Hubbard, *Thorax* **2011**, *66*, 462–467.
- [14] A. Datta, C. J. Scotton, R. C. Chambers, *Br. J. Pharmacol.* **2011**, *163*, 141–172.
- [15] G. Hughes, H. Toellner, H. Morris, C. Leonard, N. Chaudhuri, *J. Clin. Med.* **2016**, *5*, 78.
- [16] A. B. Roberts, M. B. Sporn, R. K. Assoian, J. M. Smith, N. S. Roche, L. M. Wakefield, U. I. Heine, L. A. Liotra, V. Falangat, J. H. Kehrl, A. S. Faucit, *Proc. Natl. Acad. Sci. U. S. A.* **1986**, *83*, 4167–4171.
- [17] M. J. Anderton, H. R. Mellor, A. Bell, C. Sadler, M. Pass, S. Powell, S. J. Steele, R. R. A. Roberts, A. Heier, *Toxicol. Pathol.* **2011**, *39*, 916–924.
- [18] B. Alberts, A. Johnson, J. Lewis, M. Raff, K. Roberts, P. Walter, *Molecular Biology of the Cell*, Garland Science, New York, **2002**.
- [19] D. Sheppard, *Eur. Respir. J.* **2008**, *17*, 157–162.
- [20] G. Saini, J. Porte, P. H. Weinreb, S. M. Violette, W. A. Wallace, T. M. McKeever, G. Jenkins, *Eur. Respir. J.* **2015**, *46*, 486–494.
- [21] G. S. Horan, S. Wood, V. Ona, J. L. Dan, M. E. Lukashev, P. H. Weinreb, K. J. Simon, K. Hahm, N. E. Allaire, N. J. Rinaldi, J. Goyal, C. A. Feghali-Bostwick, E. L. Matteson, C. O'Hara, R. Lafyatis, G. S. Davis, X. Huang, D. Sheppard, S. M. Violette, *Am. J. Respir. Crit. Care Med.* **2008**, *177*, 56–65.
- [22] R. J. D. Hatley, S. J. F. Macdonald, R. J. Slack, J. Le, S. B. Ludbrook, P. T. Lukey, *Angew. Chem. Int. Ed. Engl.* **2018**, *57*, 2–26.
- [23] C. H. Maden, D. Fairman, M. Chalker, M. J. Costa, W. A. Fahy, N. Garman, P. T. Lukey, T. Mant, S. Parry, J. K. Simpson, R. J. Slack, S. Kendrick, R. P. Marshall, *Eur. J. Clin. Pharmacol.* **2018**, *74*, 701–709.
- [24] J. Adams, E. C. Anderson, E. E. Blackham, Y. W. R. Chiu, T. Clarke, N. Eccles, L. A. Gill, J. J. Haye, H. T. Haywood, C. R. Hoenig, M. Kausas, J. Le, H. L. Russell, C. Smedley, W. J. Tipping, T. Tongue, C. C. Wood, J. Yeung, J. E. Rowedder, et al., *ACS Med. Chem. Lett.* **2014**, *5*, 1207–1212.
- [25] P. A. Procopiou, N. A. Anderson, J. Barrett, T. N. Barrett, M. H. J. Crawford, B. J. Fallon, A. P. Hancock, J. Le, S. Lemma, R. P. Marshall, J. Morrell, J. M. Pritchard, J. E. Rowedder, P. Saklatvala, R. J. Slack, S. L. Sollis, C. J. Suckling, L. R. Thorp, G. Vitulli, et al., *J. Med. Chem.* **2018**, *61*, 8417–8443.
- [26] N. A. Anderson, B. J. Fallon, J. M. Pritchard, **2014**, WO 2014/154725 A1.
- [27] N. A. Anderson, I. B. Campbell, M. H. J. Campbell-Crawford, A. P. Hancock, S. Lemma, S. J. F. Macdonald, **2014**, WO2016/046230 A1.
- [28] M. T. Robak, M. A. Herbage, J. A. Ellman, *Chem. Rev.* **2010**, *110*, 3600–3740.
- [29] M. Mineno, Y. Sawai, K. Kanno, N. Sawada, H. Mizufune, *J. Org. Chem.* **2013**, *78*, 5843–5850.
- [30] In a parallel series of experiments using ethyl bromoacetate in the Reformatsky reaction, the ethyl ester analogue of amine **9** was Boc-protected and determined to be >97% e.e. by HPLC on a chiral stationary phase (Figure S2, Supporting Information).
- [31] L. Jiang, D. J. Morgans, G. Bergne, C. Chen, H. Li, P. Andre, R. L. Halcomb, J. Cha, T. Hom, **2018**, WO2018/49068 A1.
- [32] B. Sreedhar, G. T. Venkanna, K. B. Shiva Kumar, V. Balasubrahmanyam, *Synthesis* **2008**, 795–799.
- [33] S. B. Ludbrook, S. T. Barry, C. J. Delves, C. M. T. Horgan, *Biochem. J.* **2003**, *369*, 311–318.
- [34] R. J. Young, D. V. S. Green, C. N. Luscombe, A. P. Hill, *Drug Discov. Today* **2011**, *16*, 822–830.
- [35] M. Kansy, F. Senner, K. Gubernator, *J. Med. Chem.* **1998**, *41*, 1007–1010.
- [36] X. Dong, N. E. Hudson, C. Lu, T. A. Springer, *Nat. Struct. Mol. Biol.* **2014**, *21*, 1091–1096.
- [37] J. Xiong, T. Stehle, R. Zhang, A. Joachimiak, M. Frech, S. L. Goodman, M. A. Arnaut, *Science* **2002**, *296*, 151–155.
- [38] P. C. D. Hawkins, A. G. Skillman, G. L. Warren, B. A. Ellingson, M. T. Stahl, *J. Chem. Inf. Model.* **2010**, *50*, 572–584.
- [39] M. McGann, *J. Chem. Inf. Model.* **2011**, *51*, 578–596.